Osher's Scheme for Real Gases

Ambady Suresh*
Sverdrup Technology, Inc., NASA Lewis Research Center, Cleveland, Ohio 44135
and
Meng-Sing Liou†
NASA Lewis Research Center, Cleveland, Ohio 44135

An extension of Osher's approximate Riemann solver to include gases with an arbitrary equation of state is presented. By a judicious choice of thermodynamic variables, the Riemann invariants are reduced to quadratures that are then approximated numerically. The extension is rigorous and does not involve any further assumptions or approximations over the ideal-gas case. Numerical results are presented to demonstrate the feasibility and accuracy of the proposed method.

I. Introduction

SEVERAL split-flux formulas are known for upwind differencing of the inviscid terms in computational fluid dynamics (CFD) codes for ideal gases. The generic formula is due to Gudonov[1] and is based on the exact solution of Riemann's initial-value problem. Numerical efficiency is achieved by introducing approximations and simplifications to the Riemann solution, which lead to various split-flux formulas. For ideal gases, the most popular "approximate Riemann solvers" are the flux-vector splittings by Steger and Warming[3] and Van Leer[4] and the flux-difference splittings by Roe[5] and Osher.[6]

Only in the last few years has intensive research been undertaken to deal with gases described by general equations of state, which arise in high-temperature, chemically reacting, equilibrium, or nonequilibrium flows. Colella and Glaz[2] extended the numerical procedure for obtaining the exact Riemann solution to gases with a general equation of state. Extensions of some of the above ideal-gas flux splitting schemes have been done with care and rigor while maintaining consistency and avoiding unnecessary assumptions or approximations (e.g., Refs. 7-10). Although these splitting formulas differ in detail, there does not seem to be any serious conceptual difficulty in carrying out the extensions of Steger-Warming (SWS), Van Leer (VLS), and Roe (RS) schemes to gases with a general equation of state. This is, however, not the case for the Osher splitting (OS), for which no such extension exists, for reasons described below.

Among the four splitting formulas, SWS and RS are not continuously differentiable across the transition points where eigenvalues change sign. Consequently, SWS has a "glitch" at a sonic point and RS allows an "expansion shock," even though some fixes are possible. In contrast, the VLS and OS are continuously differentiable across transition points and are known to lead to smoother solutions near the transition points. In addition, the smoothness of the numerical flux is a definite advantage in achieving convergence, e.g., in the framework of multigrid.[11] However, the VLS is known to yield rather smeared contact discontinuities, thus requiring many more grid points for resolving viscous shear layers. Hence, the best choice of the above four splittings seems to be the Osher scheme that has the following desirable properties: 1) smoothness at transition points, 2) stationary and sharp contact discontinuity/shocks, 3) satisfaction of the entropy condition, and 4) robustness. Thus, the immediate question arises as to how the OS can be extended to real gases with general equations of state. This is the objective of the present research.

A major difficulty in extending the Osher scheme to real gases arises because the Osher scheme makes explicit use of the Riemann invariants that do not exist in closed form for real gases. An approximation may be attempted by locally freezing the "equivalent γ," which may not be continuous in the flowfields. This can lead to considerable error in reacting flows.

In the remainder of this paper, we first discuss the equation of state for a real gas and some related thermodynamic quantities. Section III then presents the basic first-order explicit Osher scheme. A crucial element of this scheme is the determination of the intermediate states and sonic points, which are described in Sec. IV. Incorporation of these split-flux formulas in a Total Variation Diminishing (TVD) algorithm and application to a few typical problems is described in Sec. V. Finally, we close with a few remarks of a general nature in Sec. VI.

II. Equation of State

In this paper, we restrict ourselves to the gas in chemical equilibrium, described by the general equation of state (EOS):

$$p = p(\rho, e) \tag{1}$$

where ρ is the density and e the internal energy of the gas. From thermodynamic principles, it is possible to calculate any thermodynamic variable for each pair of state quantities (ρ, e). As will be seen later, the key toward extending the Osher scheme to real gases is to use the pressure p and the entropy s

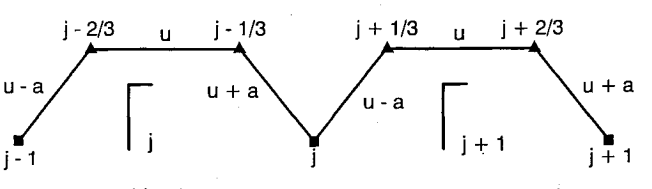

Fig. 1 Schematic representation of the integration paths for the Osher scheme using the natural order.

Received Nov. 8, 1989; presented as Paper 90-0397 at the AIAA 28th Aerospace Sciences Meeting, Reno, NV, Jan. 8-11, 1990; revision received March 30, 1990.

*Senior Research Engineer. Member AIAA.
†Senior Scientist, Internal Fluid Mechanics Division. Member AIAA.

as independent thermodynamic variables. In these variables, the Riemann invariants are reduced to quadratures and the scheme can be extended rigorously without any additional approximations. However, since the conservation laws directly provide variables (ρ,u,e), some inversion procedure to go from (ρ,e) to (p,s) variables and vice versa is clearly required.

In practice, the EOS is generated as a single, least-squares fit of the results of some chemical kinetic routine with all relevant species included. Typically, after scaling the results, a set of 10–50 basis functions of the independent variables is used to obtain a least-squares fit of all of the required dependent variables. A direct way to invert the EOS is to generate two curve fits, one using (ρ,e) as independent variables and another using (p,s) as independent variables. Although this would be computationally inexpensive, the disadvantage is that thermodynamic relations such as the first law would be satisfied only to the accuracy of the curve fits. Thus, we reject this procedure in favor of an approximate procedure based on the first law of thermodynamics that uses only the original curve fit in the (ρ,e) variables, as described below.

The inversion problem is encountered in two settings: the first in determining the fluxes at the intermediate points and the second in determining the flux at the sonic points. In both, the problem is to find (ρ,e) given p along an isentrope through a grid point U_L. In practice, first-order approximations work in most cases. The procedure begins by approximating ρ by

$$\rho = \rho_L + (p-p_L)/(a^2)_L$$

and if $(\rho-\rho_L)/\rho_L \le 10$, then

$$e = e_L + p_L/\rho_L^2$$

For large gradients, an additional step is necessary. In this case,

$$e = e_L + (\rho-\rho_L)p_1/\rho_1^2$$

where $p_1 = p(\rho_1,e_1)$ and

$$\rho_1 = (\rho+\rho_L)/2$$

$$e_1 = e_L + (\rho_1-\rho_L)p_L/\rho_L^2$$

which is a two stage Runge-Kutta scheme for e.

A critical parameter in all upwind schemes is the speed of sound:

$$a^2 = p_\rho + pp_e/\rho^2 \tag{2}$$

Here and throughout this paper, subscripts are used to denote partial derivatives; e.g., p_e denotes the partial derivative of p with respect to e while holding ρ fixed. Since the EOS is a single curve fit, it is essentially C^∞ so that a^2 is a smooth function of (ρ,e).

III. Construction of Flux Differences

To illustrate the construction of the Osher split-flux formula for real gases, we consider the one-dimensional Euler equations:

$$\frac{\partial U}{\partial t} + \frac{\partial F(U)}{\partial x} = 0 \tag{3}$$

where

$$U = [\rho,\rho u,\rho E]^t$$

$$F = [\rho u,\rho u^2 + p,(\rho E + p)u]^t$$

with $E = e + u^2/2$ as the total energy.

Let the EOS be expressed as $p = p[\rho(U),e(U)]$. The Jacobian matrix of the flux A is

$$A = \begin{pmatrix} 0 & 1 & 0 \\ A_{21} & u(2-p_e/\rho) & p_e/\rho \\ A_{31} & H-u^2p_e/\rho & u(1+p_e/\rho) \end{pmatrix} \tag{4}$$

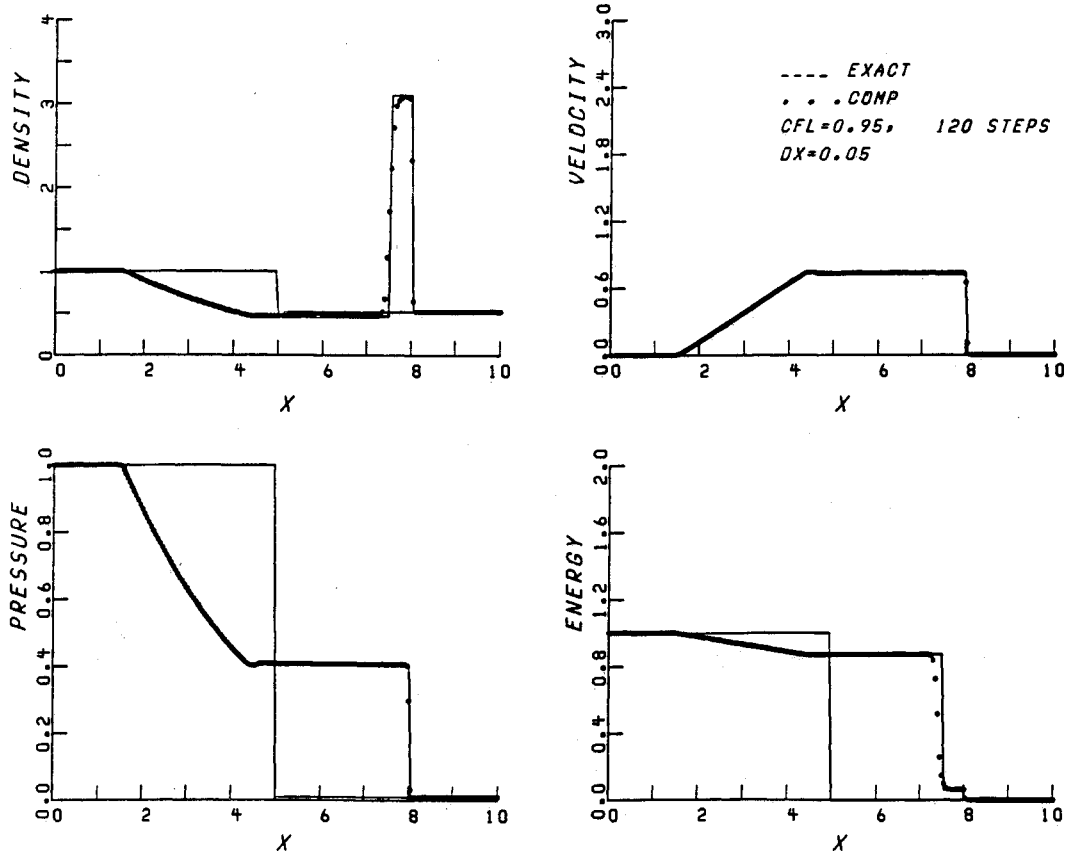

Fig. 2 Shock tube problem for equilibrium air: TVD scheme, Osher split.

where

$$A_{21} = -u^2(2 - p_e/\rho)/2 + p_\rho - p_e e/\rho$$

$$A_{31} = u[-H + u^2 p_e/2\rho + p_\rho - p_e e/\rho]$$

and the quantity $H = E + p/\rho$ is the specific total enthalpy.

The eigenvalues

$$\lambda(A) = u - a, \quad u, \quad u + a \tag{5a}$$

are used to identify the subpaths in the state-space integration, to be discussed later. The right eigenvectors associated with λ_k are

$$e_1 = [1, u - a, H - ua]^t, \quad e_2 = [1, u, H - (\rho/p_e)q^2]^t$$

$$e_3 = [1, u + a, H + ua]^t \tag{5b}$$

An eigenvalue is said to be linearly degenerate if

$$\frac{\partial \lambda_k}{\partial U} \cdot e_k = 0$$

and genuinely nonlinear otherwise. A small calculation shows that λ_2 is linearly degenerate and λ_1 and λ_3 are genuinely nonlinear if

$$-\left[\frac{\partial^2 p}{\partial \rho^2}\Big|_s\right] - \frac{a}{\rho} \neq 0$$

Hence λ_1 and λ_2 are genuinely nonlinear if the EOS is convex. Genuine nonlinearity is required both for the existence of solutions to the Riemann problem and for the uniqueness of the sonic points in the Osher scheme, as discussed below. Since the matrix A has a complete set of eigenvectors, it can be readily diagonalized by a similarity matrix S whose column vectors are the right eigenvectors of A:

$$A = S\Lambda S^{-1}, \quad \text{diag}\Lambda = \lambda(A) \tag{6}$$

where

$$S = [e_1, e_2, e_3] \tag{7}$$

In the first-order explicit Osher scheme, Eq. (3) is discretized as

$$U_j^{n+1} = U_j^n - \frac{\Delta t}{\Delta x}\left[\int_{\Gamma_j} A^+ dU + \int_{\Gamma_{j+1}} A^- dU\right] \tag{8}$$

where

$$A^+ = S\Lambda^+ S^{-1}, \quad \text{diag}\Lambda^+ = \max(\lambda_k, 0)$$

$$A^- = S\Lambda^- S^{-1}, \quad \text{diag}\Lambda^- = \Lambda - \Lambda^+ \tag{9}$$

The integration path Γ_j goes from U_{j-1} to U_j and consists of three subpaths piecewise parallel to the three eigenvectors with two intermediate states $U_{j-2/3}$ and $U_{j-1/3}$ in between, as depicted in Fig. 1. If τ represents an arc length along a subpath, then

$$\Gamma_j^k: \frac{dU}{d\tau} = e_k \tag{10}$$

Various orderings are possible, but we will use the path such that Γ_j begins at U_{j-1}, goes from U_{j-1} to $U_{j-2/3}$ along a curve (Γ_j^1) whose tangent is the eigenvector e_1, then goes from $U_{j-2/3}$ to $U_{j-1/3}$ along a curve (Γ_j^2) parallel to e_2, and then from $U_{j-1/3}$ to U_j along a curve (Γ_j^3) tangent to e_3. (Also see Fig. 1.)

This path has several interesting properties. First, the decomposition of Γ_j into Γ_j^k is locally unique since the eigenvectors are linearly independent. Furthermore, the eigenvalue λ_k is either a constant or a monotone function on the subpath Γ_j^k depending on whether λ_k is linearly degenerate or genuinely nonlinear. This implies that if λ_k changes sign over Γ_j^k, then there is a unique point on Γ_j^k where λ_k is zero. Such points are called sonic points.

The main advantage of choosing such a path is that once the intermediate states $U_{j-2/3}$ and $U_{j-1/3}$ and the sonic points (if any) are known, the integrals of Eq. (8) can be evaluated in closed form. For example,

$$\int_{\Gamma_j} A^+ dU = \int_{U_{j-1}}^{U_{j-2/3}} A^+ dU + \int_{U_{j-2/3}}^{U_{j-1/3}} A^+ dU + \int_{U_{j-1/3}}^{U_j} A^+ dU \tag{11}$$

where it follows from Eq. (10) and Eq. (9) that

$$\int_{U_{j-1}}^{U_{j-2/3}} A^+ dU = F(U_{j-2/3}) - F(U_{j-1}) \quad \text{if } \lambda_1(U_{j-2/3}) > 0, \quad \lambda_1(U_{j-1}) > 0$$

$$= F(U_{j-2/3}) - F(U_{j-2/3}^s) \quad \text{if } \lambda_1(U_{j-2/3}) > 0, \quad \lambda_1(U_{j-1}) \leq 0$$

$$= F(U_{j-2/3}^s) - F(U_{j-1}) \quad \text{if } \lambda_1(U_{j-2/3}) \leq 0, \quad \lambda_1(U_{j-1}) > 0$$

$$= 0 \quad \text{if } \lambda_1(U_{j-2/3}) \leq 0, \quad \lambda_1(U_{j-1}) \leq 0 \tag{12}$$

where $U_{j-2/3}^s$ is the unique sonic point on Γ_j^1. Similar results hold for Γ_j^3 with λ_3 replacing λ_1 in Eq. (12). Since λ_2 is linearly degenerate, it follows that

$$\int_{U_{j-2/3}}^{U_{j-1/3}} A^+ dU = F(U_{j-1/3}) - F(U_{j-2/3}) \quad \text{if } \lambda_2(U_{j-1/3}) = \lambda_2(U_{j-2/3}) > 0$$

$$= 0 \quad \text{if } \lambda_2(U_{j-1/3}) = \lambda_2(U_{j-2/3}) \leq 0 \tag{13}$$

Expressions for the integral over Γ_{j+1} in Eq. (8) are mirror images of Eqs. (12) and (13) with positive and negative signs interchanged.

Other orderings that preserve all of the properties mentioned above are possible. The order given above, wherein the left state is connected to the right state via increasing eigenvalues, is called natural order, meaning that the sequence used is what occurs naturally in the solution to the Riemann problem. The natural order has the advantage that it returns the exact solution if more than one wave is present. On the other hand, the reverse order, where the sequence is in decreasing eigenvalues, has the advantage that the existence of a steady shock is easy to prove. Both orderings admit steady contacts. However, our experience, as well as that of others, has shown that the natural order is much more robust.

Second-order accuracy is obtained, as usual, by adding suitably limited correction terms to the first-order numerical flux implied by Eq. (8). These terms have the effect of making the scheme second-order accurate in smooth (nonextremal) regions of the flow. Since this procedure is more or less standard, it will not be repeated here. It is thus clear that once the intermediate states and the sonic points have been obtained on Γ_{j+1} and Γ_j, the Osher scheme can be implemented

easily. For ideal gases, the intermediate states and sonic points are obtained by equating the closed-form Riemann invariants along the subpaths. For real gases, the question lies in how the intermediate states and sonic points can be obtained for which no closed-form Riemann invariants exist. This question is addressed in the next section.

IV. Intermediate States and Sonic Points

To obtain the intermediate states and sonic points, we switch to the nonconservative variables (p,u,s) and assume $\rho = \rho(p,s)$ and $a = a(p,s)$. First, let us consider the intermediate points. From Eq. (10), a lengthy but straightfoward calculation shows that on Γ_j^1 we have

$$\int_{p_{j-1}}^{p_{j-2/3}} \frac{dp}{\rho(p,s_{j-1})a(p,s_{j-1})} + (u_{j-2/3} - u_{j-1}) = 0$$

$$s_{j-2/3} = s_{j-1} \tag{14}$$

on Γ_j^2 we have

$$u_{j-2/3} = u_{j-1/3}$$
$$p_{j-2/3} = p_{j-1/3} \tag{15}$$

and on Γ_j^3 we have

$$\int_{p_j}^{p_{j-1/3}} \frac{dp}{\rho(p,s_j)a(p,s_j)} - (u_{j-1/3} - u_j) = 0$$

$$s_j = s_{j-1/3} \tag{16}$$

In the integrals above, the entropy s is held fixed during the integration and appears only as a parameter. Adding Eqs. (14) and (16) and using Eq. (15), we get a single equation for $p^* = p_{j-2/3} = p_{j-1/3}$:

$$\int_{p_j}^{p^*} \frac{dp}{\rho(p,s_j)a(p,s_j)} + \int_{p_{j-1}}^{p^*} \frac{dp}{\rho(p,s_{j-1})a(p,s_{j-1})} - u_{j-1} + u_j = 0 \tag{17a}$$

Since $\rho,a > 0$, the left-hand side of Eq. (17a) is a monotone increasing function of p^* and thus for small $|U_j - U_{j-1}|$ a unique solution to p^* exists. Once p^* is known, $u^* = u_{j-2/3} = u_{j-1/3}$ can be obtained from either Eq. (14) or Eq. (16). With p^* and u^* known, the intermediate states are given by $U_{j-2/3} = (p^*,u^*,s_{j-1})$ and $U_{j-1/3} = (p^*,u^*,s_j)$.

In practice, base-point approximations suffice for Eq. (17a). p^* is obtained from

$$\frac{(p^* - p_j)}{(\rho a)_j} + \frac{(p^* - p_j)}{(\rho a)_{j-1}} - u_{j-1} + u_j = 0 \tag{17b}$$

Once p^* is known, u^* is obtained by a similar first-order approximation of either Eq. (14) or Eq. (16). Once p^* and u^* are known, two EOS inversions are performed to obtain the fluxes $F_{j-2/3}$ and $F_{j-1/3}$ at the intermediate points.

As long as the error in the quadrature is subdominant compared to the overall discretization error, no further loss of accuracy is incurred. Thus, making use of exact Riemann invariants as proposed by Osher is not required. Furthermore, for an ideal gas, the quadrature evaluation is comparable to the calculation involving exponents. This is exactly the key observation that makes the extension to nonideal gases possible.

Next we turn to the determination of the sonic points. Assume that conditions are such that a sonic point $U_{j-2/3}^s$ exists on Γ_j^1. Then

$$u_{j-2/3}^s = a_{j-2/3}^s = a(p_{j-2/3}^s, s_{j-1}) \tag{18}$$

Using Eq. (18) in Eq. (14) gives

$$\int_{p_{j-1}}^{p_{j-2/3}^s} \frac{dp}{\rho(p,s_{j-1})a(p,s_{j-1})} - u_{j-1} = -a(p_{j-2/3}^s, s_{j-1}) \tag{19a}$$

which is a nonlinear equation for $p_{j-2/3}^s$. If the EOS is convex, $a_p > 0$ everywhere, so that the left-hand side of Eq. (19a) is a monotone increasing function of $p_{j-2/3}^s$ while the right-hand side of Eq. (19a) is a monotone decreasing function. Thus, the

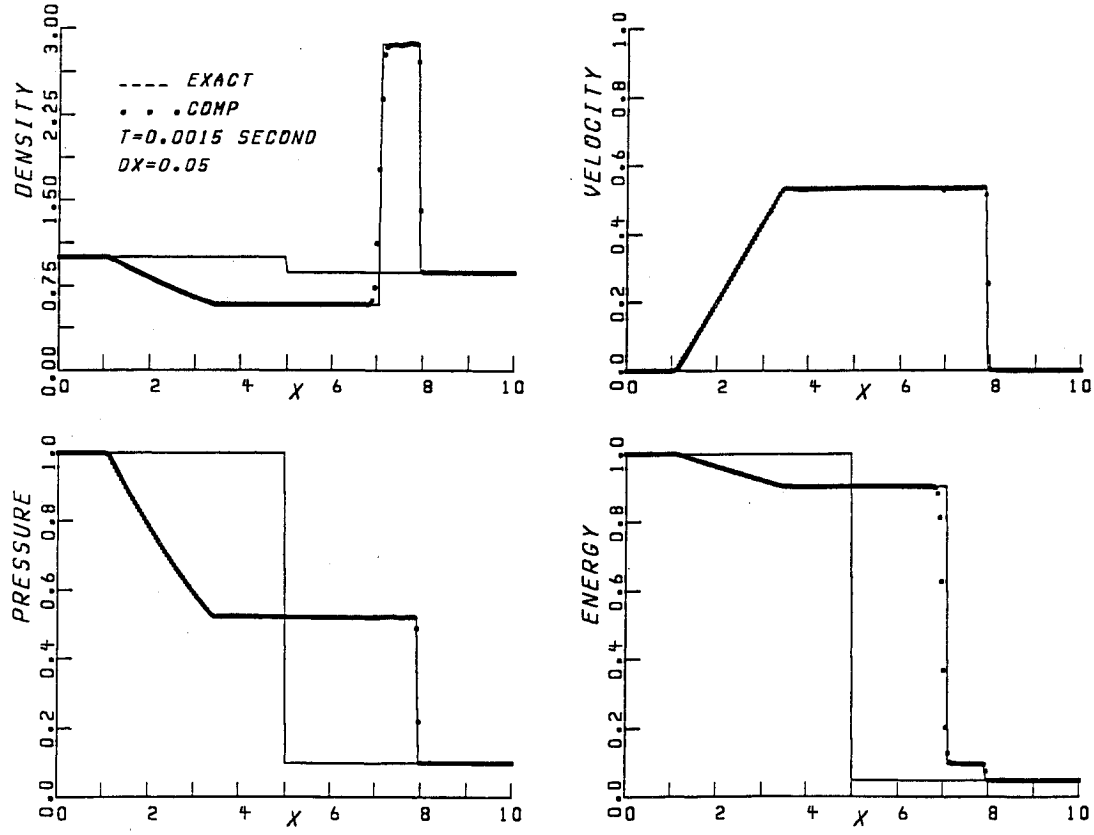

Fig. 3 Shock tube problem using the natural order: SOO problem, Osher scheme.

sonic point is unique. The requirement of convexity is also apparent from the fact that the eigenvalues are genuinely nonlinear only under this assumption. Once $p^s_{j-2/3}$ is known, then $u^s_{j-2/3}$ can be obtained from Eq. (18). Thus, the sonic point is completely specified by $U^s_{j-2/3} = (p^s_{j-2/3}, u^s_{j-2/3}, s_{j-1})$. In practice, base-point approximations suffice to solve Eq. (19a), which was approximated as

$$\frac{p^s_{j-2/3} - p_{j-1}}{(\rho a)_{j-1}} - u_{j-1} = -a_{j-1} - a_p \,|_s (p^s_{j-2/3} - p_{j-1}) \quad (19b)$$

Once $p^s_{j-2/3}$ is known, $u^s_{j-2/3}$ is obtained from the right-hand side of Eq. (19b). The derivative a_p can be obtained from

$$a^2 a_p \,|_s = a_\rho \,|_e + p a_e \,|_\rho / \rho^2$$

where the derivatives on the right-hand side were obtained by differentiating the EOS. Once $p^s_{j-2/3}$ and $u^s_{j-2/3}$ are known, then a single EOS inversion is carried out to obtain the flux at the sonic point.

In retrospect, the intermediate states and sonic points in the general case are obtained by transforming to the (p,u,s) variables where the Riemann invariant can be expressed as a simple quadrature. Since the quadrature need only be as accurate as the spatial discretization, this is not computationally intensive. In fact, when the quadrature was applied to ideal gases, the computational effort was more or less the same as using the Riemann invariants, since the latter involve exponents. Also, the existence of stationary shocks and contacts can be proved using the definitions given above in the same manner as in Ref. 12.

Other approaches for gaining efficiency and accuracy are possible. One approach is to successively differentiate Eq. (10) along the various subpaths and obtain the intermediate and sonic points to higher order in τ. However, the first-order approximations mentioned below worked quite well even for very extreme shock-tube problems.

V. Numerical Test

Extensive tests over a wide range of flow conditions were conducted to validate the accuracy of the present formulation, including some extreme cases of one-dimensional unsteady shock-tube and steady-nozzle problems. The performance of the present scheme for real gases is compared with the exact solution; some typical results are given in this paper.

The Euler equations are integrated using the explicit Lax-Wendroff scheme. To obtain a crisp and monotone shock representation, the TVD scheme[13] utilizing the above split formula to result in upwinding is employed. The super-Bee limiter is used for steepening the contact discontinuity.

The computational grid consists of 200 equally spaced points for the shock-tube problem. The initial conditions used are as follows.

For $0 \le x \le 5$:

$$p_4 = 100 \text{ atm}, \qquad T_4 = 9000 \text{ K}, \qquad u_4 = 0$$

For $5 \le x \le 10$:

$$p_1 = 1 \text{ atm}, \qquad T_1 = 300 \text{ K}, \qquad u_1 = 0$$

The EOS is generated using the widely referred program by Gordon and McBride[14] for equilibrium air in the range 250 K $\le T \le$ 12,000 K, 0.1 atm $\le p \le$ 100 atm, in which 17 species are included. With over 3600 sets of state points, a least-squares fit for pressure is obtained with 20 basis functions of (ρ,e). The resulting standard deviation does not exceed 0.2%; the maximum error occurs, as expected, on the boundary.

The results of the computation, which used the natural order, are shown in Fig. 2. The exact solution was calculated by iterating for the pressure downstream of the shock until the velocities on both sides of the contact surface match. The agreement with the exact solution is in general excellent. We also note that the contact discontinuity is slightly sharper than previous results using Roe's splitting.[8]

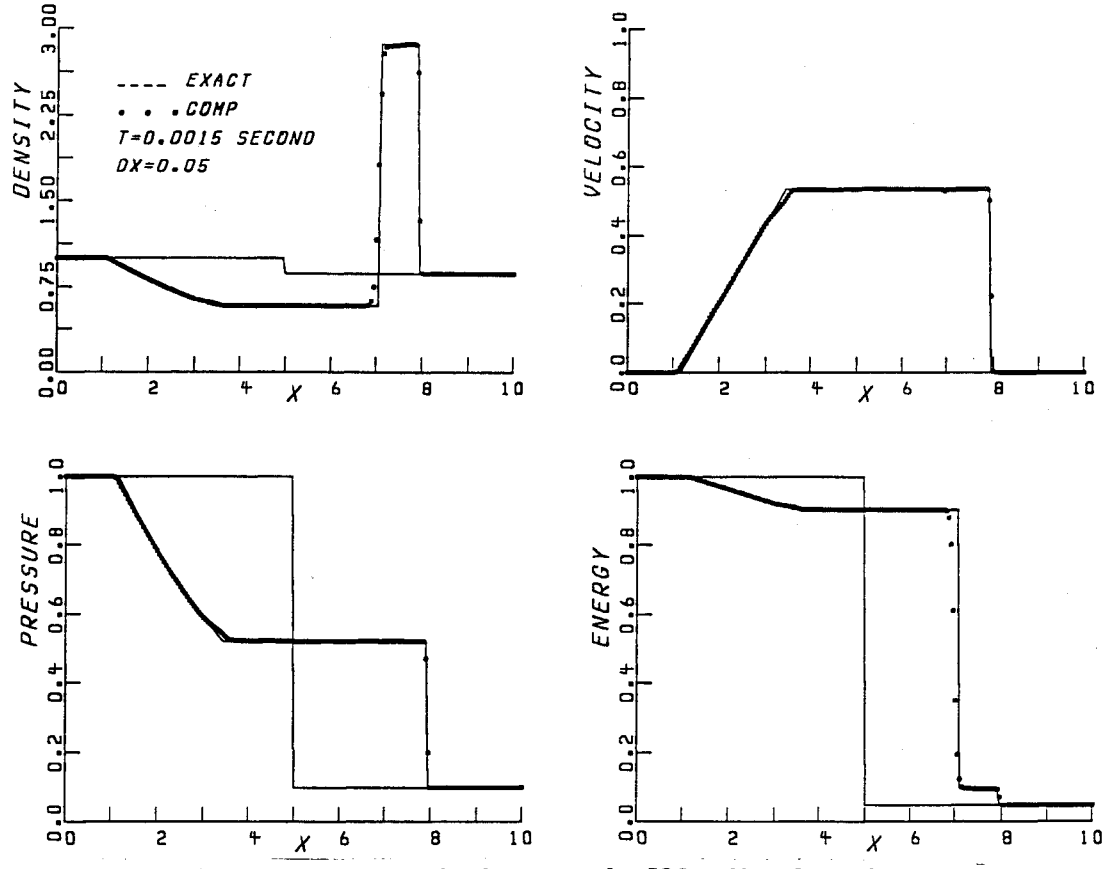

Fig. 4 Shock tube problem using the reverse order: SOO problem, Osher scheme.

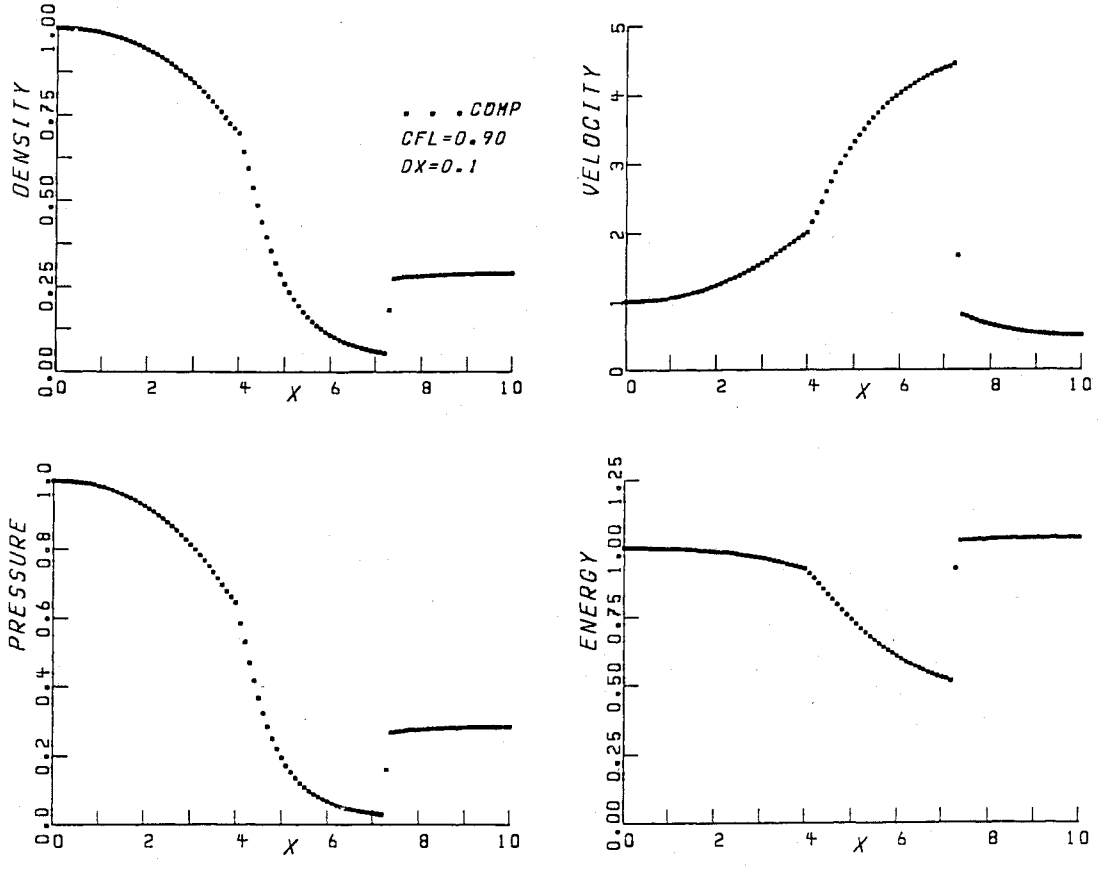

Fig. 5 Convergent-divergent nozzle problem for equilibrium air: Osher scheme, normal order.

Figures 3 and 4 compare solutions obtained using the natural order and reverse order, respectively, for a milder shock-tube problem with $p_2 = 10$ atm, $T_2 = 1500$ K, and other parameters as given above. Note the "dogleg" at the tail of the expansion fan ($x = 3.1$) for the reverse order, which vanishes when the natural order is used. In general, the natural order was more robust over a wide range of test problems. The natural ordering also seems to be the one used in current practice.[15]

Figure 5 shows the results of pressure, velocity, density, and internal energy, normalized by entrance conditions, for the problem of steady flow through a convergent-divergent nozzle with an embedded normal shock. For this case, the grid consisted of 100 equally spaced points and the Covrant-Friedrichs-Lewy (CFL) used was 0.9. The area distribution of the nozzle was

$$A(x) = 5.5 - 4.5\cos[(x-4)\pi/6], \qquad 4 \le x \le 10$$

$$A(x) = 1.2 - 0.2\cos[(x-4)\pi/4], \qquad x \le 4$$

The entrance conditions were $p_0 = 2.02 \times 10^6$ Pa, $T_0 = 6000$ K, and $u_0 = 787.08$ m/s. The results show crisp and monotone profiles across the shock, with the steady shock resolved in one intermediate point.

The approximations given above minimize the number of EOS evaluations, as these are generally expensive. For every pair of points u_{j-1}, u_j to compute $f_{j+1/2}$ the number of EOS evaluations depend on the data. If the gradients are moderate and a sonic point does not exist, then no additional EOS evaluations are needed. If the gradients are moderate but a sonic point exists, then two additional calls to the EOS are required. If gradients are large and a sonic point does not exist, two additional calls to EOS are required. Finally, if gradients are large and a sonic point exists, then four additional EOS evaluations are required.

A typical shock-tube calculation using the above scheme took about 7-10% more CPU time as compared to a Roe solver without an entropy fix. The scheme is thus quite efficient and competitive with other upwind schemes. Further increases in efficiency are possible by better approximations and innovative programming.

VI. Concluding Remarks

In this paper, we have shown how the Osher scheme may be extended in a straightforward manner to real gases by a judicious choice of thermodynamic variables. It is gratifying to note that the extension is rigorous and does not involve any further assumptions or approximations over the ideal-gas case. This is in contrast to the extension of the Roe scheme to real gases, where the extension is non-unique.

As the EOS is generated as an arbitrary curve fit, the convexity condition is not a priori satisfied. However, we did not find this to be a problem in our computations. In the determination of the sonic points, second derivatives of the EOS are needed. This is one reason we decided against using piecewise curve fits for the EOS, as smoothness is lost at the interfaces.

The issue regarding the ordering of the subpaths is similar to that for the ideal-gas case. Using the reverse order, the existence of a shock with a one-point transition follows from the results of Ref. 12. However, no such result is available with the natural order. Nevertheless, we obtained much better results using the natural order, with dramatic improvements in certain cases.

Acknowledgments

The first author was supported by the NASA Lewis Research Center under Contract NAS-25266 with T. J. Benson as monitor. The authors would like to thank Jian-Shun Shuen for several illuminating discussions and the use of his EOS curve fits for air.

References

[1]Godonov, S. K., *Mat. Sb.,* Vol. 47, 1959, p. 271.
[2]Collela, P., and Glaz, H. M., *Journal of Computational Physics,* Vol. 59, 1985, p. 264.
[3]Steger, J. L., and Warming, R. F., *Journal of Computational Physics,* Vol. 40, 1981, p. 263.
[4]Van Leer, B., *Lecture Notes in Physics,* Springer-Verlag, New York, Vol. 170, 1982 p. 507.
[5]Roe, P. L., *Journal of Computational Physics,* Vol. 43, 1981, p. 357.
[6]Osher, S., *Mathematical Studies,* North Holland, Amsterdam, Vol. 47, 1981, p. 179.
[7]Vinokur, M., and Liu, Y., "Equilibrium Gas Flow Computations II: An Analysis of Numerical Formulations of Conservation Laws," AIAA Paper 88-0127, 1988.
[8]Liou, M.-S., van Leer, B., and Shuen, J. S., *Journal of Computational Physics* (to be published).
[9]Glaister, P., *Journal of Computational Physics,* Vol. 74, 1988, p. 382.
[10]Larrouturou, B., and Fezoui, L., "On The Equations of Multi-Component Perfect or Real Gas Inviscid Flow," Nonlinear Hyperbolic Problems, *Lecture Notes in Mathematics,* edited by Carasso, Charrier, Hanovzet, and Joly, Springer-Verlag, Heidelberg, 1989.
[11]Hemker, P. W., and Koren, B., "Defect Correction and Nonlinear Multigrid for the Steady Euler Equations," *Lecture Series on Computational Fluid Dynamics,* Von Karman Inst. for Fluid Dynamics, 1988.
[12]Osher, S., and Solomon, F., *Mathematics of Computation,* Vol. 38, 1982, p. 339.
[13]Liou, M.-S., "A Generalized Procedure for Constructing an Upwind Based TVD Scheme," AIAA Paper 87-0355, 1987.
[14]Gordon, S., and McBride, B. J., NASA SP-273, 1976.
[15]Osher, S., private communication, 1989.